

Active species in Ar-N₂-H₂-CH₄ flowing microwave discharges for hard coatings

A. Ricard, H. Malvos and H. Michel*

LPGP - CNRS - Bat 212, Université Paris-Sud 91405 ORSAY - FRANCE

* LSGS - CNRS - Ecoles des Mines - Parc de Saurupt 54 042 NANCY - FRANCE

Abstract:

High quality iron nitrided layers have been obtained by using flowing microwave post-discharges in Ar-N₂-H₂-CH₄ mixtures.

The afterglow is characterized by emission of spectral bands from N₂ (B, V' = 11-8) and CN (B, V' = 7) radiative states, resulting from N + N and C + N recombination reactions, respectively. The N and C atom densities have been determined by NO titration for N atoms and from band intensities of the spectra emitted by the N + N and C + N reactions. In conditions of 40 Torr - 120 watts, 2.45 GHz discharges with Ar - 11% N₂ - 5x10⁻⁵CH₄, it has been determined [N] ~ 5x10⁻¹⁵ cm⁻³ and [C] ~ 10¹³ cm⁻³ at a time of 10⁻¹ sec. in the post discharge.

With such N and C atom densities in the post-discharge, thick ε - Fe₂3 N coatings (20-22 μm) have been produced, without oxide layers, for treatment times of 3 hours and a substrate temperature of 550° C.

1. Introduction

A growing interest in the use of flowing nitrogen post-discharges has recently appeared in the field of surface coating processes. For instance, coatings of Fe₄N-γ' of 4-6 μm thickness (with a steel substrate temperature of 840K and a processing time of one hour) have been obtained in a microwave (2450 MHz, 70 W) induced flowing post-discharge generated from an Ar-3% N₂ gas mixture. It has been established that the thickness of γ' coating is increasing with N- atom densities which have been measured by NO titration [1].

The afterglow of the Ar-N₂ flowing discharge is characterized by the emission of the N₂(B, V' = 11 - 8) radiative states, resulting from the recombination of N-atoms. Also in the afterglow, a strong emission of CN coming from impurities has been observed. Particularly, a strong intensity of the CN(B, 7 - X, 7) band results from the C + N recombination process [2].

In the present paper, production of N atoms in the Ar-N₂-H₂ and Ar-N₂-CH₄ post-discharges is first analysed from the afterglow coming from the N₂(B, V' = 11-8) states. The C-atom densities have been determined in the Ar-N₂-CH₄ post-discharge from N-atom densities which is measured by NO

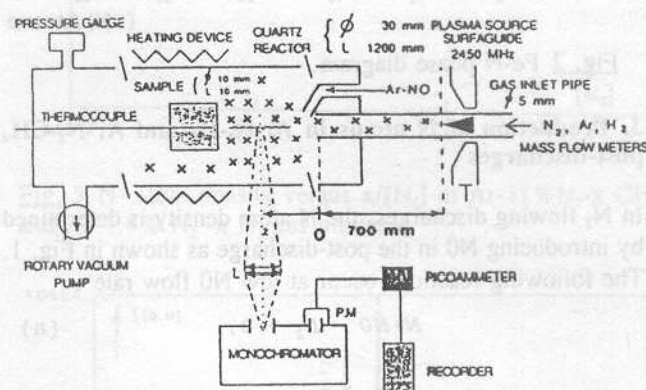


Fig. 1 Microwave post-discharge reactor.

titration and from measurements of band intensities which are emitted by the N + N and C + N recombination reactions. Finally, the chemical composition and thickness of nitrided layers on iron substrates are correlated to the N and C atom densities in the post-discharge.

2. The microwave plasma reactor in flowing Ar-N₂-H₂-CH₄ gases

The microwave post-discharge reactor used for steel surface nitriding is reproduced in Fig. 1. The plasma is initiated in a 0.5 cm diam. quartz tube with a surfaguide structure [3]. The post-discharge runs into a reactor of a diam. 3 cm and length of 120 cm at a distance of 70 cm from the surfaguide structure. The Fe-0.1% C samples are cylinders of a diam. of 1 cm and length of 1 cm. They are heated at the nitriding temperature with a conventional heating device. As indicated by the phase diagram of Fig.2, ε, γ', and α layers can be obtained at 840 K and the austenite γ layer is obtained in addition at T = 880K. The sample temperature is monitored by a chromel alumel thermocouple whose hot junction is placed 2 mm under the treated surface. The afterglow has been analyzed by emission spectroscopy using a Jobin-Yvon HR 640 spectrometer with a 1 200 groove diffraction grating and a Hamamatsu R 636 photomultiplier connected to a picoammeter and a chart recorder.

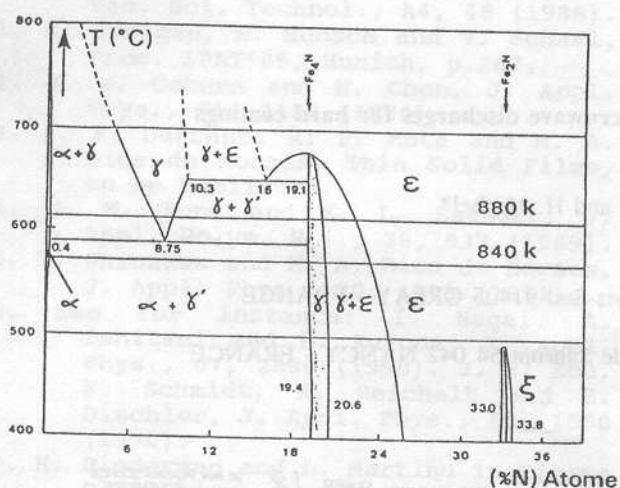
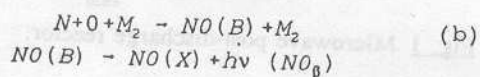
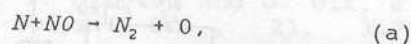


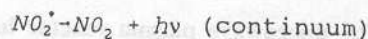
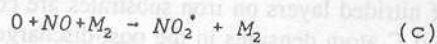
Fig. 2 Fe-N phase diagram.

3. Production of N atoms in Ar-N₂-H₂ and Ar-N₂-CH₄ post-discharges

In N₂ flowing discharges, the N atom density is determined by introducing NO in the post-discharge as shown in Fig. 1. The following reactions occur at low NO flow rate :



At high NO flow rate, all the N atoms being recombined, it follows :



The change from NO_β to the NO₂^{*}-continuum is produced when the NO and N flow rates are equal.

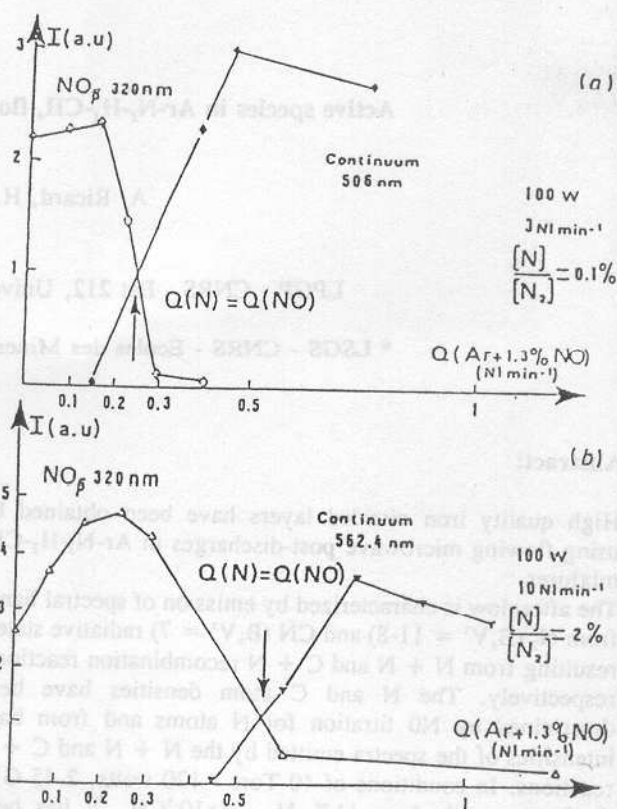
The variation of the NO_β band head intensity at 320 nm as a function of Ar-1.3% NO flow rate is reported in Fig. 3a at 23 Torr in N₂ and in Fig. 3b, at 200 Torr in Ar-3% N₂. The decrease of NO_β intensity is followed by a tenuous

green emission of NO₂^{*} which has been detected at 506 and 562.4 nm (Fig. 3).

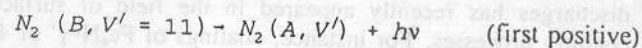
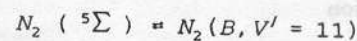
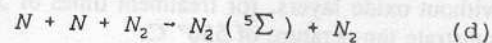
The extinction point corresponds to the intersection of NO_β and NO₂^{*} curves from which the N atom density is

obtained: N/N₂ = 0.1% in N₂ discharge at 23 Torr and N/N₂ = 2% in Ar-3% N₂ discharge at 200 Torr [4].

In N₂ afterglow, the emission spectra is characterized by first positive N₂(B, V'-A, V'') emission whose high vibrational levels are out of equilibrium with a maximum on N₂(B, V' = 11) for Ar-(>10%) N₂ gas mixtures (Cf. Fig. 4). This maximum value is the result of the N atom


 Fig. 3 Intensities of NO_β and NO₂^{*} bands versus NO flow rate for N titration by NO.

recombination following the reaction :



where the N₂(B, V' = 11) state is produced from the N₂(⁵Σ) potential curve-crossing [5].

The band intensity (I_{N₂}) from N₂(B, 11) can be written as it follows :

$$I_{N_2} = C(\lambda_1) \frac{hc}{\lambda_1} A_1 [N_2(B, 11)] \quad (1)$$

where C(λ₁) is the spectral response at λ₁ of the optical system (Cf. Fig. 1), λ₁ = 580.4 nm and A₁ = 6.2 × 10⁴ sec⁻¹ [6].

The N₂(B,11) state density is given by the following equation :

$$[N_2(B, 11)] = \frac{[N]^2 [M_2] k_1}{v_1^2 + [M_2] k_q^1} \quad (2)$$

where $C(\lambda_i)$ is the spectral response at λ_i of the optical system (Cf. Fig. 1), $\lambda_i = 580.4 \text{ nm}$ and $A_i = 6.2 \times 10^4 \text{ sec}^{-1}$ [6].

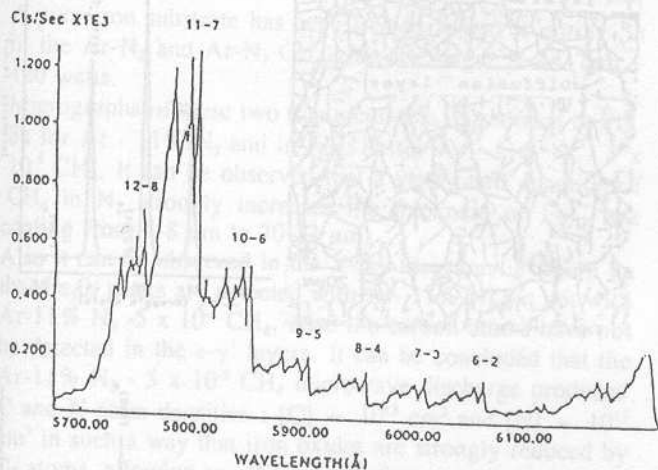


Fig. 4 I^{st} positive $N_2(B, V'-A, V'')$ intensity in $Ar(> 10\%) N_2$ post-discharge.

where $v_1^f = \sum A_{1,j} = 2.3 \times 10^5 \text{ sec}^{-1}$ and $k_q^1(Ar) = 0.2 \times 10^{-11} \text{ cm}^3 \text{ sec}^{-1}$ and $k_q^1(N_2) = 2.8 \times 10^{-11} \text{ cm}^3 \text{ sec}^{-1}$ [7].

It follows from eq. 1 and 2 that :

$$I_{N_2} = K_1 [N]^2 \quad (3)$$

where K_1 is related to the rate coefficients in eq. 1 and 2.

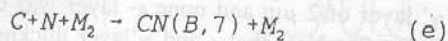
Then the N- atom density can be determined from I_{N_2}

intensity measurements after calibration by NO.

Results are reported in Fig. 5 for $Ar-N_2-H_2$ gas mixtures at a time $\Delta t = 10^{-1} \text{ sec}$ in the post-discharge. Such a decrease of N atom density with H_2 has been analysed in ref. 8 as resulting from $N_2(V) + H_2$ quenching reactions. In condition of a $N_2 - 1\% H_2$ d.c discharge with $E/N = 5 \times 10^{-16} \text{ V cm}^2$, $T_v = 4000 \text{ K}$ and $T_g = 400 \text{ K}$, the N_2 dissociation rate is less than $10^{-14} \text{ cm}^3 \text{ sec}^{-1}$, much lower than in pure N_2 discharge where it is $3 \times 10^{-10} \text{ cm}^3 \text{ sec}^{-1}$.

4. Production of C atoms in $Ar-N_2-CH_4$ post-discharges

In the blue part of the $Ar - (> 10\%) N_2$ afterglow, a strong emission of CN coming from olefin impurities has been observed as reproduced in Fig. 6 [2]. Particularly, a strong intensity of $CN(B, 7 - X, 7)$ is the result of the following recombination process :



By comparing the intensities of $CN(B, 7-X, 7)$ and $N_2(B, 11-A, 7)$ bands in the afterglow, the C- atom density can be estimated from the N- atom density obtained by NO titration. The band intensity (I_{CN}) from $CN(B, 7)$ is given by the following equation :

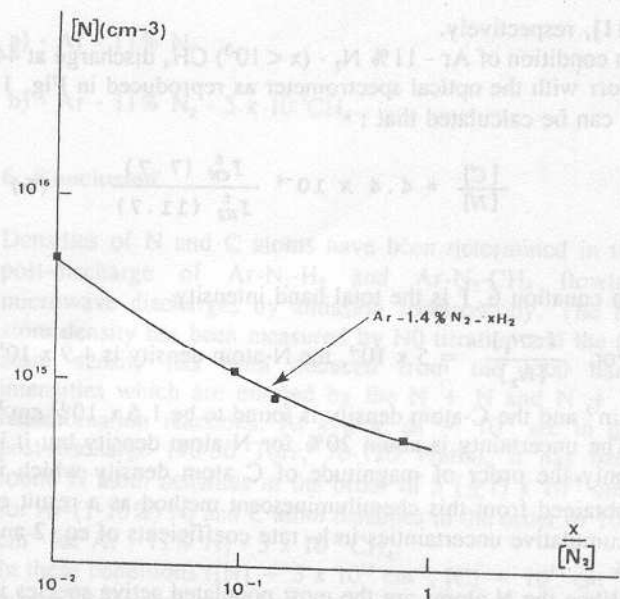


Fig. 5 N- atom density versus $x/[N_2]$ in $Ar-11\%N_2-x CH_4$ and $Ar-1.4\% N_2-x H_2$ gas mixtures.

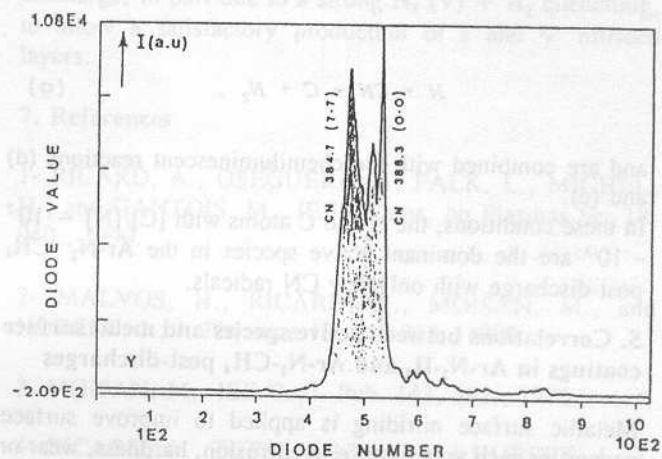


Fig. 6 $CN(B, V' - X, V'')$ emission intensity from olefin impurity in $Ar(> 10\%) N_2$ post-discharge.

$$I_{CN} = C(\lambda_2) \frac{hc}{\lambda_2} A_2 [CN(B, 7)] \quad (4)$$

where $\lambda_2 = 384.7 \text{ nm}$ and $A_2 = 2.5 \times 10^7 \text{ sec}^{-1}$ [9]. The $CN(B, 7)$ state density is given by :

$$[CN(B, 7)] = \frac{[C] [N] k_2}{v_2^f + [M_2] k_q^2} \quad (5)$$

where $v_2^f = 2.5 \times 10^7 \text{ sec}^{-1}$ and $k_q^2(Ar) = 10^{-11} \text{ cm}^3 \text{ sec}^{-1}$ [10]. The recombination rate coefficient in eq. 2 and 5 are $k_1 = 10^{-33} \text{ cm}^6 \text{ sec}^{-1}$ [4] and $k_2 = 10^{-32} \text{ cm}^6 \text{ sec}^{-1}$

[11], respectively.

In condition of Ar - 11% N₂ - (x < 10⁻³) CH₄ discharge at 44 Torr with the optical spectrometer as reproduced in Fig. 1, it can be calculated that :

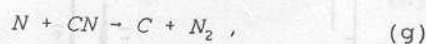
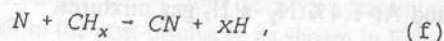
$$\frac{[C]}{[N]} = 4.4 \times 10^{-4} \frac{I_{CN}^t (7.7)}{I_{N_2}^t (11.7)} \quad (6)$$

In equation 6, I^t is the total band intensity.

For $\frac{[CH_4]}{[N_2]} = 5 \times 10^{-4}$, the N-atom density is 4.9×10^{15}

cm⁻³ and the C-atom density is found to be 1.6×10^{13} cm⁻³. The uncertainty is about 20% for N atom density but it is only the order of magnitude of C atom density which is obtained from this chemiluminescent method as a result of cumulative uncertainties in k- rate coefficients of eq. 2 and 5.

When the N atoms are the most populated active species in the post-discharge, the following chain reactions could occur [9].



and are combined with the chemiluminescent reactions (d) and (e).

In these conditions, the N and C atoms with [C]/[N] ~ 10⁻² - 10⁻³ are the dominant active species in the Ar-N₂-CH₄ post-discharge with only few CN radicals.

5. Correlations between active species and metal surface coatings in Ar-N₂-H₂ and Ar-N₂-CH₄ post-discharges

Metallic surface nitriding is applied to improve surface properties such as resistance to corrosion, hardness, wear or fatigue by the development of thin surface layers (depth of 1-10 μm) having high resistance properties. Low pressure gas discharges (1-5 Torr) are commonly used for steel surface nitriding and carburizing in industrial reactors. In such plasma treatments, the sample is usually connected as a cathode of a glow discharge in flowing N₂-H₂ and N₂-H₂-CH₄ gas mixtures.

It is to separate the contribution of ionic species such as

N₂⁺ and that the neutral active species such as N₂ (V)

vibrational excited molecules, N and C atoms, that the post-discharge reactor as reproduced in Fig. 1 has been setup.

5.1 Metal surface coatings in Ar-N₂-H₂ post-discharges

After post-discharge treatments of 1h at 840K in Ar- 1.4% N₂ at 50 Torr, a γ' layer of 4 μm with an ε layer of about 1 μm was obtained as shown in Fig. 7a. The steel substrate is very sensitive to oxidation in the temperature range of

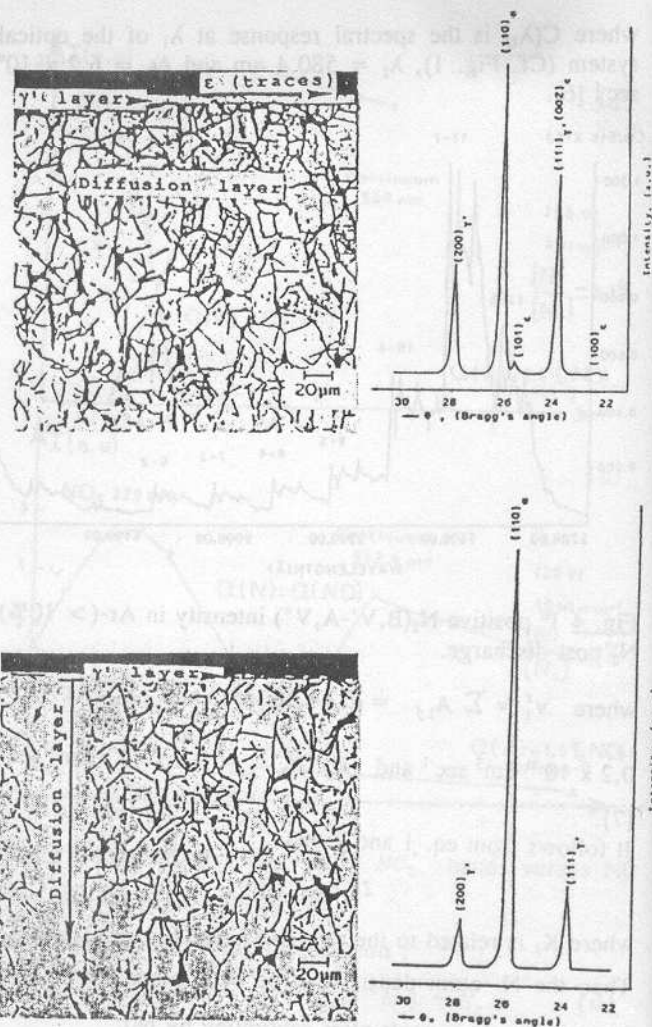


Fig. 7 Micrographs of iron - 0,1% C layers after an 1 hour post-discharge treatment at 840K in 50 Torr-70W discharges. Diffracted X-ray intensity versus Bragg's angle θ at the surface of nitrided layers :

a) Ar - 1.4% N₂ - 0.2% H₂ during the 1st 5 min. of treatment and Ar - 1.4% N₂ alone in the following.

b) Ar - 1.4% N₂ - 0.2% H₂ during all the treatment time.

nitriding, resulting in part from water and air impurities inside the reactor. Thin iron oxides as Fe₃O₄ inhibit the nitriding reaction. To avoid it, small concentrations of H₂ gas (0.2% H₂ in Ar-1.4% N₂ gas mixture) were introduced in the initial part of the treatment (2-3 min). But when H₂ flow was maintained during all the treatment time, a weaker γ' layer of 2 μm and none ε- layer was obtained as shown in Fig 7b. Note that ε and γ' layer thickness in Fig. 7a and 7b was directly determined by measurements on micrographs or from (110)α and (200)γ' intensity ratio of X diffraction pattern [1].

As shown in Fig. 5, a sharp decrease of N atoms is observed when small H₂ percentage is introduced into the Ar-N₂ discharge which can be related to a reduced γ' layer

as shown in Fig. 7b.

5.2 Metal surface coatings in Ar-N₂-CH₄ post-discharges

A pure iron substrate has been treated at 840 K during 3h in the Ar-N₂ and Ar-N₂-CH₄ post-discharges at 44 Torr - 120 watts.

Micrographs of these two treatments are reproduced in Fig. 8a for Ar - 11% N₂ and in Fig. 8b for Ar - 11% N₂ - 5 x 10⁻⁵ CH₄. It can be observed that a very small quantity of CH₄ in N₂ strongly increases the thickness of Fe_{2,3} N-ε coating from 4-8 μm to 20-22 μm.

Also it can be observed in the X-ray diagrams in figure 8a that Fe₃O₄ peaks are detected with Ar- 11% N₂ but not with Ar-11% N₂ - 5 x 10⁻⁵ CH₄. Also the carbon atoms have not been detected in the ε-γ' layers. It can be concluded that the Ar-11% N₂ - 5 x 10⁻⁵ CH₄ microwave discharge produced C and N atom densities : [C] ~ 10¹³ cm⁻³ and [N] ~ 10¹⁵ cm⁻³ in such a way that iron oxides are strongly reduced by C-atoms, allowing an efficient nitriding process (ε- layer of 20μm).

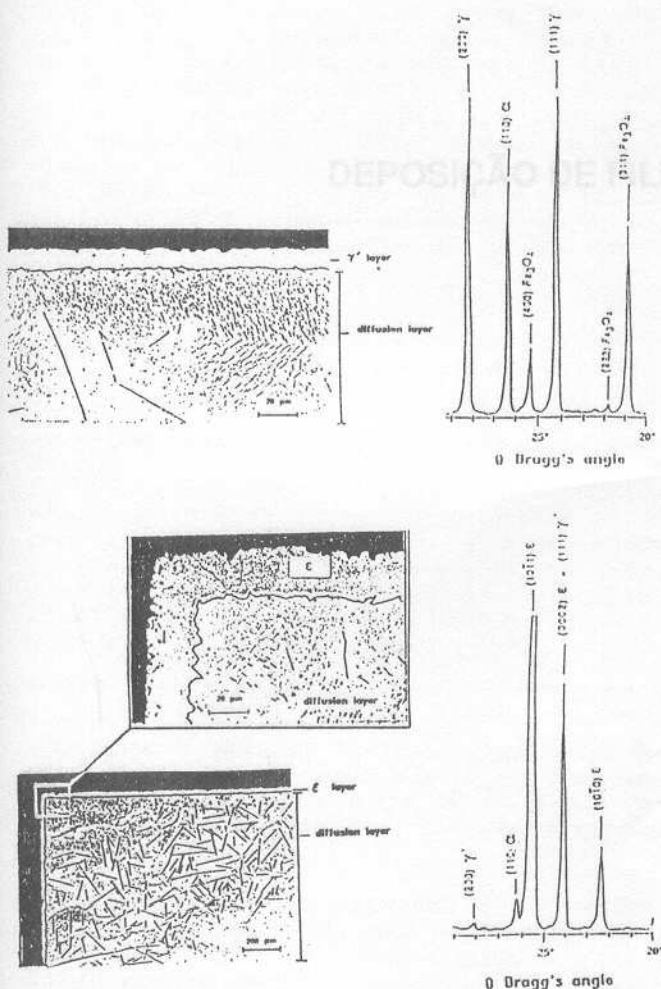


Fig. 8 Micrographs of pure Fe samples after a 3 hours post-discharge treatment at 840 K in 44 Torr - 120W discharges. Diffracted X-ray intensity versus Bragg's angle θ at the surface of nitrided layers.

a) - Ar - 11% N₂

b) - Ar - 11% N₂ - 5 x 10⁻⁵ CH₄

6. Conclusion

Densities of N and C atoms have been determined in the post-discharge of Ar-N₂-H₂ and Ar-N₂-CH₄ flowing microwave discharges by emission spectroscopy. The N-atom density has been measured by NO titration and the C-atom density has been deduced from the total band intensities which are emitted by the N + N and N + C recombination reactions. At a time $\Delta t \sim 10^{-1}$ sec in the post-discharge (40-50 Torr, 70-120 Watts), it has been found N atom densities in the order of $5 (\pm 1) \times 10^{15}$ cm⁻³ for Ar-(1-10%) N₂ and C atom densities in the order of 10^{13} cm⁻³ for Ar - 11% N₂ - 5 x 10⁻⁵ CH₄.

In these conditions ([N] ~ 5×10^{15} cm⁻³, [C] ~ 10^{13} cm⁻³), where CN radicals are destroyed by N atoms, a high quality of iron nitrided layers has been obtained : 20 μm of ε- layer without oxides for a 3 hour treatment. With Ar-N₂ - H₂ gas mixtures the N atoms are weakly produced in the flowing discharge, in part due to a strong N₂ (V) + H₂ quenching, to allow a satisfactory production of ε and γ' nitrided layers.

7. References

- 1- RICARD, A., OSEGUERA, J., FALK, L., MICHEL, H., and GANTOIS, M., IEEE Trans. on Plasmas Sc. 18, 940., 1990.
- 2- MALVOS, H., RICARD, A., MOISAN, M., and HUBERT, J., J. Physique 18, C 5-313., 1990.
- 3- MOISAN, M., IEE Conf. Pub. 143, 382., 1976.
- 4- RICARD, A., TETREAULT, J., and HUBERT, J., J. Phys. B24, 1115., 1991.
- 5- PARTRIDGE et al., J. Chem. Phys. 88, 3174., 1988.
- 6- LOFTHUS, A., KRUPENIE, P.H., J. Phys. Chem. Ref. Data 6, 113., 1977.
- 7- CAMPBELL, I.M., and THRUSH, B.A., , Proc. Roy. Soc A 296, 201., 1967.
- 8- LOUREIRO, J., Xth ESCAMPIG, 30 (Orleans), 1990. To be published in J. Phy. B (1992).
- 9- RICARD, A., MALVOS, H., BORDELEAU, S., and HUBERT J., ISPC - 10 (Bochum), 1991.
- 10- TERESHCHENKO, E.N., and DODOVA, N.Y., Optics and Spectry. 39, 435., 1975.

11- WASHIDA, N., KLEY, D., BECKER, K.H., and GROTH, W., J. Chem. Phys. 63, 4230., 1975.

Fig. 1 Microwave post-discharge reactor.

Fig. 2 Fe-N phase diagram.

Fig. 3 Intensities of NO_p and NO_2^* bands versus NO flow rate for N titration by NO .

Fig. 4 I^a positive $N_2(B,V'-A,V'')$ intensity in Ar-($> 10\%$) N_2 post-discharge.

Fig. 5 N- atom density versus $x/[N_2]$ in Ar-1.4% N_2 - x H_2 gas mixtures.

Fig. 6 $CN(B,V' - X,V'')$ emission intensity from olefin impurity in Ar-($> 10\%$) N_2 post-discharge.

Fig. 7 Micrographs of iron - 0,1% C layers after an 1 hour post-discharge treatment at 840K in 50 Torr-70W discharges. Diffracted X-ray intensity versus Bragg's angle θ at the surface of nitrided layers :

a) Ar - 1.4% N_2 - 0.2% H_2 during the I^a 5 min. of treatment and Ar - 1.4% N_2 alone in the following.

b) Ar - 1.4% N_2 - 0.2% H_2 during all the treatment time.

Fig. 8 Micrographs of pure Fe samples after a 3 hours post-discharge treatment at 840 K in 44 Torr - 120W discharges. Diffracted X -ray intensity versus Bragg's angle θ at the surface of nitrided layers.

a) - Ar - 11% N_2

b) - Ar - 11% N_2 - $5 \times 10^{-5} CH_4$